Nuclear Engineering and Design 241 (2011) 2416–2424

Contents lists available at ScienceDirect

Nuclear Engineering and Design

journal homepage: www.elsevier.com/locate/nucengdes

Mechanical properties of steel fiber reinforced reactive powder concrete following exposure to high temperature reaching 800 °C

Yuh-Shiou Tai [a,*], Huang-Hsing Pan [b], Ying-Nien Kung [b]

[a] Department of Civil Engineering, ROC Military Academy, Kaohsiung, Taiwan, ROC
[b] Department of Civil Engineering, Kaohsiung University of Applied Sciences, Kaohsiung, Taiwan, ROC

ARTICLE INFO

Article history:
Received 16 October 2009
Received in revised form 30 March 2011
Accepted 1 April 2011

ABSTRACT

This study investigates the stress–strain relation of RPC in quasi-static loading after an elevated temperature. The cylinder specimens of RPC with φ 50 mm × 100 mm are examined at the room temperature and after 200–800 °C. Experimental results indicate that the residual compressive strength of RPC after heating from 200–300 °C increases more than that at room temperature, but, significantly decreases when the temperature exceeds 300 °C. The residual peak strains of RPC also initially increase up to 400–500 °C, then decrease gradually beyond 500 °C. Meanwhile, Young's modulus diminishes with an increasing temperature. Based on the regression analysis results, this study also develops regression formulae to estimate the mechanical properties of RPC after an elevated temperature, thus providing a valuable reference for industrial applications and design.

1. Introduction

When the concrete structure is subject to high temperatures, the most important effects on concrete are: dehydration of cement paste, porosity increase, thermal expansion, thermal creep and thermal spalling due to excessive pore pressure (Bazant and Kaplan, 1996; Noumowé et al., 2009). Additionally, inconsistent heat deformation between the mortar and coarse aggregate decreases the strength. The mechanical properties of fiber reinforced concrete (FRC) after high temperatures have received considerable attention in recent years (Reis et al., 2001; Chen and Liu, 2004; Li et al., 2004; Poon et al., 2004; Georgali and Tsakiridis, 2005; Husem, 2006; Arioz, 2007; Sideris et al., 2009; El-Dieb, 2009). Based on the results, they concluded that FRC has various excellent properties as a composite material; for instance, flexural, tensile and shear strength, toughness, impact resistance, crack resistance and resistance to frost damage can be improved by the use of steel fiber. SFRC has been commonly used in industry for tunnel lining and road paving. However, the main contribution of a small percentage of fibers is to increase the toughness of concrete. Throughout a concrete mix with steel fibers distributed in all directions, micro cracks which appear due to shrinkage or applied loading, intersect with steel fibers which block their growth and provide higher tensile capacity. Although steel fiber may not offer any obvious advantage from a fire-endurance point of view, previous work (Hannant, 1978; Lau and Anson, 2006) has shown that steel fibers can affect the spread of cracking, and hence potentially improve the performance of concrete, after exposure to high temperatures. To combat explosive spalling, several investigations by researchers have been carried out, which revealed that the application of polypropylene (PP) fibers in concrete may considerably reduce the amount of spalling for HPC at elevated temperatures. Both experimental and theoretical studies have shown (Hammer, 1992; Nishida and Yamazaki, 1995; Chan et al., 1999; Atkinson, 2004) that at high temperatures, PP fibers melt and create channels through which the water vapour pressure built-up within HPC as temperatures rise is released. This release of the vapour pressure significantly reduces the spalling tendency of HPC under fire conditions (Kalifa et al., 2001).

Significant advances in high-performance concrete (HPC) are largely attributed to technological applications, especially high-range water reducers. HPC is superior to conventional concrete in terms of density and micro-structure via a refined mixing scheme, subsequently yielding a higher strength, workability and durability. Based on a composite material developed by Richard and Cheyrezy (1994, 1995), reactive powder concrete (RPC) is characterized by its material's uniformity that is increased by eliminating coarse aggregate and using silica sand with a maximum particle size of 400 μm. Additionally, concrete density is increased by selecting optimum particle size components. Doing so significantly reduces the porosity and markedly increases compressive strength and durability, giving it both a high strength and high performance (Richard and Cheyrezy, 1994, 1995; Cheyrezy et al., 1995; Zanni et al., 1996). Cheyrezy et al. (1995) observed the working mechanism of RPC's high strength and durability while studying its microstructure.

* Corresponding author. Tel.: +886 7 7456290; fax: +886 7 7104697.
E-mail addresses: ystai@cc.cma.edu.tw, ys.tai@msa.hinet.net (Y.-S. Tai).

0029-5493/$ – see front matter © 2011 Elsevier B.V. All rights reserved.
doi:10.1016/j.nucengdes.2011.04.008

Table 1
Properties of cement and silica fume.

Material	Cement	Silica fume
Chemical composition (%)		
SiO_2	22.60	90
Al_2O_3	3.75	1
Fe_2O_3	4.55	1
CaO	63.15	0.4
MgO	2.17	1
SO_3	1.88	
C		2
Loss on ignition, L.O.I.	0.62	3

Based on use of nuclear magnetic resonance technology, Zanni et al. (1996) investigated the hydration and pozzolanic reaction inside a specimen that received 20 °C and 250 °C heat curing. According to their results, the amount of silica fume that participated in hydration was directly proportional to the heat curing temperature. Bayard and Plé (2003) found that the distribution of steel fibers in RPC significantly affects its mechanical behavior. Additionally, the distribution could be adjusted via a modified casting procedure to enhance its mechanical performance. Chan and Chu (2004) elucidated how silica fume content affects the cohesion between the RPC base material and steel fibers, indicating that cohesive results are optimum when the silica fume contents ranged from 20–30%. Previous studies (Zhang et al., 2008; Wang et al., 2008; Tai, 2009a,b) on the mechanical behavior of RPC under dynamic and impact loads found that RPC had enhanced impact resistance and energy absorption capabilities with respect to conventional concrete and high strength concrete.

RPC is a more appropriate construction material for military facilities and important structures than conventional concrete owing to its enhanced workability and mechanical properties. However, an exhaustive literature review indicated that the mechanical behavior of RPC under high temperatures has seldom been studied. Therefore, this study elucidates the mechanical properties of RPC with various fiber contents after withstanding high temperatures. Results of this study provide a valuable reference for future construction applications and design.

2. Experimental methods

2.1. Materials

Cement used in this study was ordinary Portland cement that conforms to ASTM Type II. This medium sulfate-resisting cement has a low content of calcium aluminates C_3A. Used in this study as a mineral addition, dry non-compacted silica fume has a silicon dioxide content of 90%, specific gravity of 2.2, and a specific surface of 18–20 m^2/g. Table 1 lists the chemical compositions of the cement and SF. Quartz sand with a maximum particle size of 0.6 mm was also used in this study. Crushed crystalline quartz powder is a critical component in heat-treated RPC concretes. Reactivity during heat treatment reaches maximum for an average particle size ranging from 5 to 25 μm. An average particle size of 10 μm was used. Additionally, an attempt was made to improve slurry at low water–cement ratios by using a high performing water-reducing agent. The chemical ingredient in the agent, i.e. acrylic graft polymer anionic high molecular surfactant, complies with ASTM C 494 Types G. The admixture has a light-brownish color, with a specific gravity of 1.07–1.13. Corrugated steel fibers were made from cold drawn low-carbon steel. The fiber length was 12 mm and the diameter was 0.175 mm; therefore, the aspect ratio of the fibers (l/d) was 69. Table 2 lists the details of the mix proportions.

2.2. Experimental procedure

This study examined the residual strength and deformation performance of RPC after withstanding high temperatures on 120 φ50 mm × 100 mm concrete cylinder specimens. Table 2 lists the mixture components of various specimens. In this table, different groups of specimens vary in steel fiber content by volume of concrete; in addition, specimen with 1%, 2% and 3% steel fiber are labeled RPCF1, RPCF2 and RPCF3, respectively. After casting, specimens were covered with a plastic membrane to prevent moisture evaporation, followed by storage at 25 °C for 48 h. The specimens were then de-molded and placed in a thermostat-controlled water tank at 90 °C for 7 days of curing; thereafter, they were placed under high temperatures. Eight temperatures used in this study to examine the initial and residual mechanical behavior of specimens for comparison are 200 °C, 300 °C, 400 °C, 500 °C, 600 °C, 700 °C, 800 °C and 25 °C (nonheated) as the control group. Each group contained five specimens that underwent an uniaxial compression test. A K-type thermometer was buried in each specimen during production to monitor the specimen's internal temperature and ensure that it reaches a specific temperature. RPC has an extremely high density and holds large amounts of water after undergoing high temperature water curing. Therefore, to prevent the specimen spalled when heated (i.e. excessive pore pressure caused by water vapourization), the specimens were dried under 110 °C for at least 7 days before undergoing heat treatment to minimize the water contents. After the specimens reached the target temperature, heating was stopped and the specimens were left in the furnace to cool down naturally. Finally, specimens were taken out the following day and installed with extensometers on both ends for qusi-static mechanical testing.

2.3. Heating regime

The heating equipment used in this study is a high temperature electric furnace with internal space dimensions of 300W × 300H × 300D (mm), maximum temperature of 1204 °C and a maximum heating speed of 30 °C/min. The ASTM E119 standard heating curve was adopted for the fire test to simulate actual conditions. However, during heat treatment, all specimens spalled after heated within a range of 400–500 °C (Fig. 1). We speculate that this phenomenon is attributed to free water inside the specimens that could not be eliminated during the early pre-heating stage, coupled with the higher density of RPC than that of conventional concrete. Next, an attempt was made to clarify the mechanical properties of RPC after high temperatures from a fire, while preventing specimens spalling due to temperature stress caused by the high heating speed. The heating speed was decelerated to 2 °C/min, a constant temperature was maintained for 30 min after every increase of 200 °C to ensure consistent heating conditions, and, finally, a constant temperature was maintained for 30 min after the target temperature (200 °C, 300 °C, 400 °C, 500 °C, 600 °C, 700 °C and 800 °C) was reached.

Table 2
Concrete mix proportions (kg/m^3).

Specimen no.	$w/(c+sf)$	Water	Cement	Silica fume	Quartz powder	Quartz sand	Superplasticizer	Steel fiber
RPCF1	0.19	180	714	216	252	918	36	80
RPCF2	0.19	180	714	216	252	891	36	160
RPCF3	0.19	180	714	216	252	865	36	240

Fig. 1. RPC specimens spalled during ASTM standard fire test.

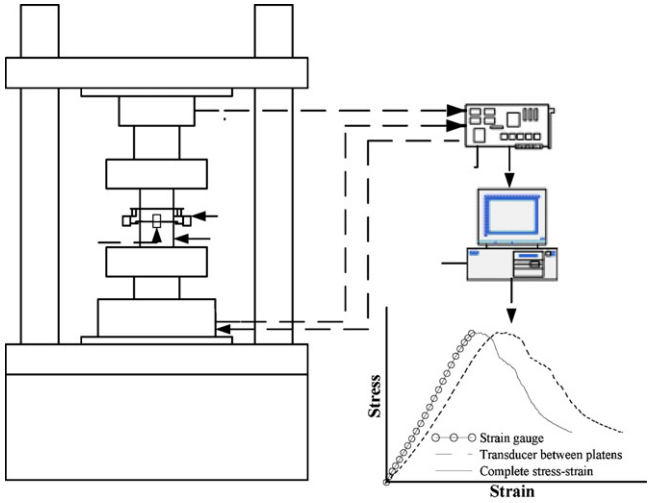

1. specimen; 2. extensometer; 3. strain gauge; 4. actuator
5. load cell; 6. controler; 7. data registering and analyzing apparatus

Fig. 2. Schematic of MTS quasi-static mechanical test system.

2.4. Mechanical testing method

The uniaxial compression test was performed using a 1000 kN MTS universal material testing machine, in which the complete stress–strain curve of RPC after high temperatures was determined by using displacement control and a loading speed of 0.03 mm/min. Fig. 2 illustrates the mechanical testing equipment and data processing procedures.

As concrete is a brittle material, when loaded to failure strength, various failure modes often make it difficult to determine axial deformation. Therefore, by incorporating the method developed by Mansur et al. (1995), this study compares the effects of adjustments to the flexibility of the testing equipment and the end-zone effect with actual deformation, as measured by an extensometer to obtain the stress–strain curve of specimen after failure.

3. Results and discussion

Results of a series of tests are discussed below with respect to appearance and color change, failure mode, and stress–strain curve characteristics of RPC after high temperatures.

3.1. Appearance and color change

The specimens appeared to change in color after a high temperature due to chemical reactions. Cracks also appeared between the cement paste and steel fibers due to their various thermal expansion coefficients. Additionally, steel fibers at the surface of specimen underwent oxidation after exposed to high temperatures, subsequently producing black carbon particles that were absorbed by the concrete. Concrete with steel fibers thus had a relatively darkish color.

Fig. 3 summarizes the results of high temperature tests on RPC. At 200 °C, the appearance and color of RPC specimens were the same as those at room temperature. At 300 °C, the RPC specimens turned to a grayish yellow color. At 400 °C, small cracks began to appear and the specimens turned to a grayish brown color. When the temperature reached 500 °C, chemical reactions occurred and the bound water separated, in addition, the number of cracks increased. At 600 °C, cracks at the specimen surface expanded and the specimen turned a darkish gray color. When

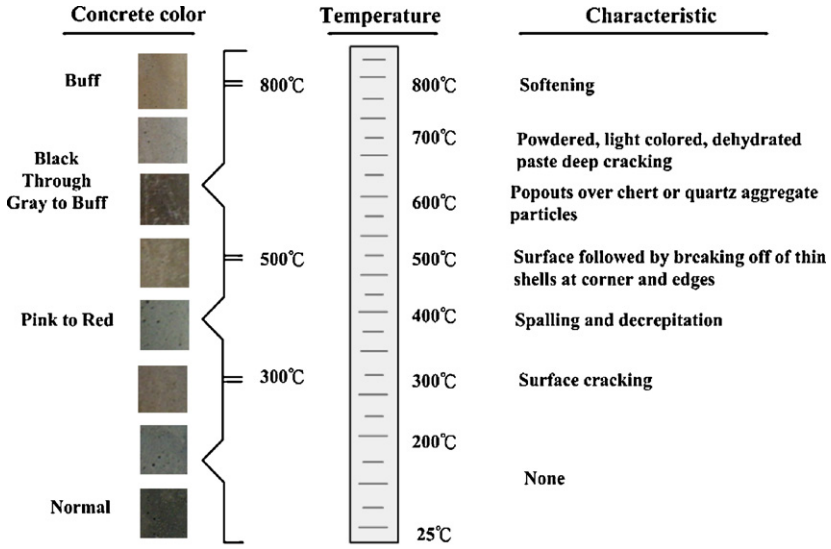

Fig. 3. Appearance characteristics and color change of RPC after a high temperature tests.

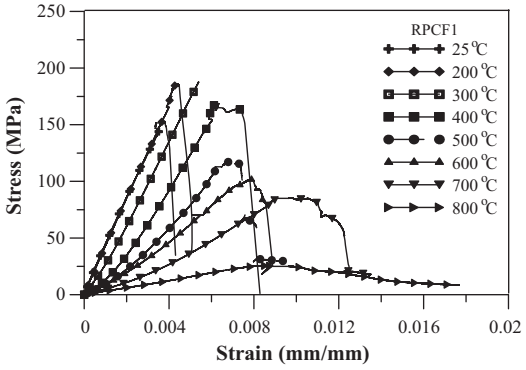

Fig. 4. Stress–strain curves of RPCF1 specimen.

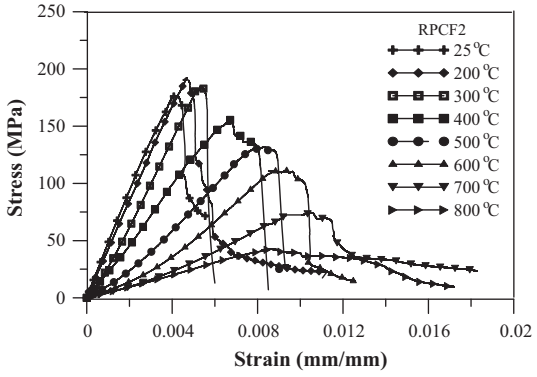

Fig. 5. Stress–strain curves of RPCF2 specimen.

temperatures reached 700–800 °C, the specimen surface became brittle and contained more pores and large cracks. Notably, specimens with different steel fiber content did not significantly differ in appearance after withstanding the same high temperature. However, specimens with a higher steel fiber content were closer to a darkish brown color after withstanding temperatures of 700 °C and above.

3.2. Stress–strain relationship

Figs. 4–6 show the stress–strain curves of RPC specimen after high temperatures, while Table 3 summarizes all high temperature

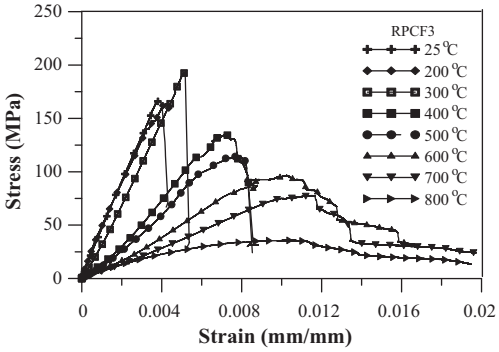

Fig. 6. Stress–strain curves of RPCF3 specimen.

mechanical property test results. Although behaving similar to conventional concrete, RPC specimens with various steel fiber contents heated to 200–300 °C have a somewhat increased compressive strength. Notably, further heating the specimens diminishes their compressive strength, increases the peak strain, and significantly decreases the modulus of elasticity. As the temperature increases, the difference between initial tangent modulus and secant modulus at peak stress decreases. For RPCF1 and RPCF2, when temperatures exceeded 500 °C, initial tangent modulus less than secant modulus and the stress–strain curve concaved upwards for the rise section before failure. This finding resembles conventional concrete, in which a large number of cracks appeared after exposed to high temperatures. When the load is first added to such specimens, their cracks would initially close up, showing a similar curve with a rapidly increasing strain and gradually increasing the stiffness (Chang et al., 2006). Owing to its relatively higher steel fiber content, RPCF3 maintained a relatively higher modulus of elasticity after a high temperature, explaining why the rise section of its stress–strain curve did not significantly concave upwards.

3.3. Compressive strength

Table 3 and Fig. 7 show the changes in the compressive strength of RPC specimen after high temperatures. For easier comparison, the value within brackets in the table is the remaining compressive strength of specimens after a high temperature, divided by their compressive strength at room temperature. According to this figure, despite increasing during early periods of heating, the compressive strength of specimens significantly decreased as heating

Table 3
Summarizes mechanical property test results.

	Compressive strength (MPa)			Elastic modulus (GPa)			Peak strain		
	RPCF1	RPCF2	RPCF3	RPCF1	RPCF2	RPCF3	RPCF1	RPCF2	RPCF3
25 °C	150.4 (1.0)[a]	168.5 (1.0)	156.5 (1.0)	43.1 (1.0)	45.6 (1.0)	46.1 (1.0)	0.0039 (1.0)	0.004 (1.0)	0.0039 (1.0)
200 °C	185.9 (1.24)	175.0 (1.04)	167.0 (1.07)	42.2 (0.98)	43.6 (0.96)	45.3 (0.98)	0.0045 (1.15)	0.0043 (1.08)	0.0041 (1.05)
300 °C	183.0 (1.22)	174.7 (1.04)	183.2 (1.17)	32.0 (0.74)	32.9 (0.72)	30.7 (0.66)	0.0054 (1.38)	0.005 (1.25)	0.0057 (1.46)
400 °C	174.8 (1.16)	137.2 (0.81)	140.4 (0.9)	25.1 (0.58)	20.2 (0.44)	18.1 (0.39)	0.0063 (1.62)	0.0069 (1.73)	0.0072 (1.85)
500 °C	107.9 (0.72)	121.5 (0.72)	128.5 (0.82)	12.8 (0.3)	13.4 (0.29)	14.9 (0.32)	0.0077 (1.97)	0.0089 (2.22)	0.0079 (2.03)
600 °C	95.4 (0.63)	101.2 (0.6)	95.9 (0.61)	10.7 (0.25)	10.1 (0.22)	9.5 (0.21)	0.0081 (2.08)	0.0091 (2.28)	0.0095 (2.44)
700 °C	87.3 (0.58)	69.3 (0.41)	76.8 (0.49)	7.6 (0.18)	6.2 (0.14)	6.9 (0.15)	0.0096 (2.46)	0.011 (2.75)	0.011 (2.82)
800 °C	27.7 (0.18)	38.0 (0.22)	36.8 (0.23)	3.6 (0.08)	4.7 (0.10)	6.2 (0.14)	0.0086 (2.21)	0.0085 (2.13)	0.0093 (2.38)

[a] The values in brackets indicate the relative increase or decrease in residual strength as compared to the control group (25 °C).

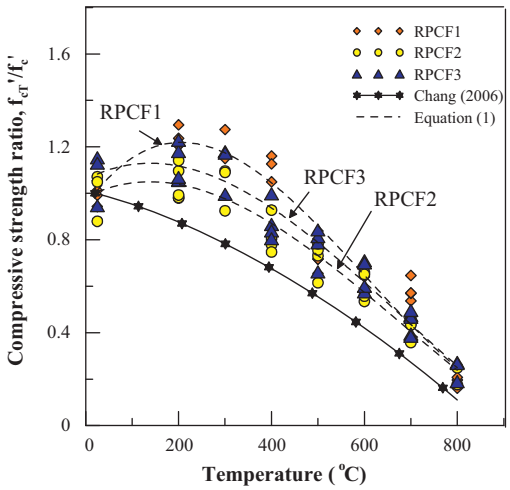

Fig. 7. Comparisons of the residual compressive strength of RPC.

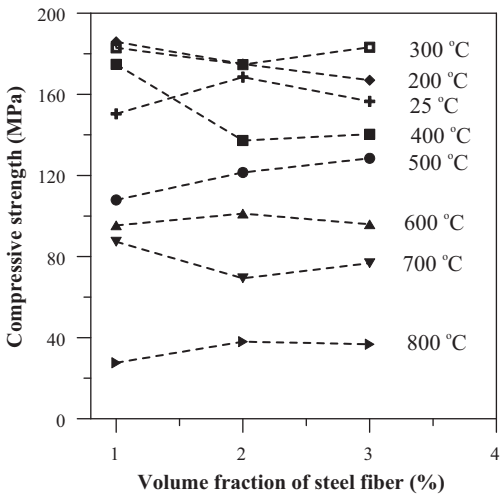

Fig. 8. Compressive strength of RPC specimens versus steel fiber content after the different temperatures.

proceeded. After RPCF1, RPCF2 and RPCF3 specimens were heated to 200 °C, their compressive strengths increased about 24%, 4% and 7%, respectively. When heated to 300 °C, their compressive strengths increased about 22%, 4% and 17%, respectively. These increases are attributed to the fact that high temperatures accelerate the pozzolanic reaction, increase the hydration products, reduce the pore size. According to Cheyrezy et al. (1995), the pozzolanic reaction of RPC specimens that underwent heat curing of 250 °C could reach 100%; the compressive strength increased as well. In contrast with RPCF1 and RPCF2, RPCF3 had a significantly higher compressive strength at 300 °C than at 200 °C. At high temperatures, although different heat capacities caused cracks to form between cement paste and steel fibers, steel fibers prevented cracks from expanding and helped to strengthen the specimens to a certain extent. Following heating of RPCF1, RPCF2 and RPCF3 to 500 °C, their compressive strength decreased about 28%and 18%, respectively. This occurrence is attributed to inconsistent expansion and shrinkage between the coarse aggregate and cement paste, subsequently incurring more cracks and reducing the compressive strength. At roughly 600 °C, crystal phase transformation cause volume expansion of the specimens to lead to dissolution of C–S–H and C–H, in which specimens decreased an average of 38% in compressive strength. At 700 °C, the compressive strength of RPCF1, RPCF2 and RPCF3 decreased by 42%, 59% and 51%, dropping to half of its original strength. Thermal expansion caused even more cracks to appear on the surface of specimens. At 800 °C, the compressive strength of RPCF1, RPCF2 and RPCF3 dropped about 82%, 78% and 77%, retaining only roughly 20% of its original strength. Notably, high temperatures (600 °C and above) severely damage the concrete structure, resulting in a serious loss of compressive strength.

Fig. 8 shows the trend in compressive strength based on steel fiber content. RPC specimens with 1% steel fiber contents have a higher compressive strength under temperatures ranging from 200–400 °C than at room temperature; compressive strength begins to decline after specimens reach 500 °C. Additionally, the compressive strength of RPC specimens with 2% and 3% steel fiber content increased significantly when heating from 200 °C to 300 °C, but began to reduce after temperatures exceeded 400 °C. We speculate that this phenomenon is attributed to inconsistent expansion and shrinkage of cement paste due to relatively higher steel fiber contents.

For RPC specimens with various steel fiber contents after high temperatures, the regression expression of the strength test results is as follows:

$$\frac{f'_{cT}}{f'_c} = \begin{cases} 0.946 + 2.855\times10^{-3}T - 8.375\times10^{-6}T^2 + 4.648\times10^{-9}T^3, & V_f = 0.01 \\ 1.059 + 1.053\times10^{-3}T - 4.223\times10^{-6}T^2 + 2.066\times10^{-9}T^3, & V_f = 0.02 \\ 0.984 + 9.782\times10^{-3}T - 3.923\times10^{-6}T^2 + 1.919\times10^{-9}T^3, & V_f = 0.03 \end{cases}, \quad 25\,^\circ\text{C} < T \le 800\,^\circ\text{C} \tag{1}$$

where f'_c and f'_{cT} represent the compressive strengths of RPC specimens under room temperature and after high temperatures, T denotes the specimen's temperature (°C), and V_f refers to steel fiber content of the specimens. The correlation coefficient R^2 for different V_f values of Eq. (1) is 0.93, 0.94 and 0.94, indicating a successful simulation. Moreover, the fire resistance properties of RPC specimens were compared with those of conventional concrete with reference to the test results of Chang et al. (2006), as shown in Fig. 7. According to this figure, in comparison with the residual strength of conventional concrete, the residual compressive strength reduction is more slowly in RPC after heating from 200 to 500 °C. But the reduction on strength after 600 °C of heating has the same trend with conventional concrete.

3.4. Peak strain

The peak strain of RPC after withstanding high temperatures and at room temperature is as shown in Fig. 9. According to Table 3 and Fig. 9, the peak strain of RPCF1, RPCF2 and RPCF3 increased 15%, 8% and 5% following heat treatment to 200 °C and increased about 38%, 25% and 46% after heated to 300 °C. Although nearly the same for temperatures under 200 °C, the peak strains of the specimens began to increase along with temperatures after 200 °C. After withstanding heat treatment at 500 °C, the peak strains of RPCF1, RPCF2 and RPCF3 increased 97%, 122% and 103%, respectively, doubling compared with room temperature. Between 400 °C and 500 °C, high temperatures induced more cracking, subsequently diminishing the compressive strength and increasing the number of peak strains rapidly. At 700 °C, the peak strains of RPCF1, RPCF2 and RPCF3 increased about 146%, 175% and 182%, reaching nearly three times that of room temperature. In the range of 600–700 °C, cracks continued to expand, subsequently causing the peak strains to rise continuously. After withstanding heat at 800 °C, the peak strains of

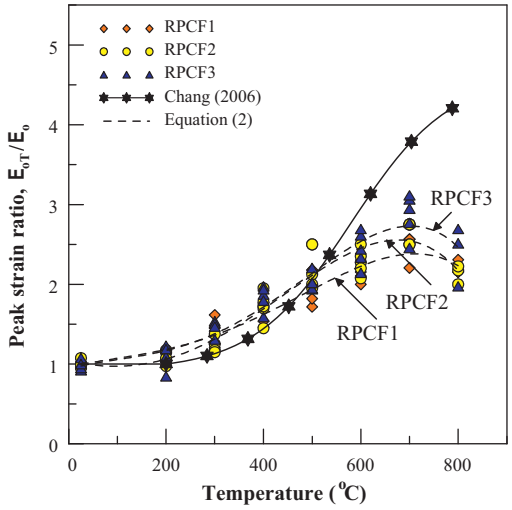

Fig. 9. Comparisons of the peak strain of RPC.

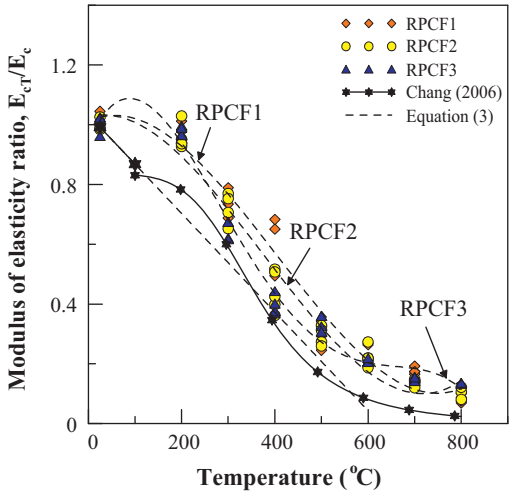

Fig. 11. Comparisons of the modulus of elasticity of RPC.

RPCF1, RPCF2 and RPCF3 increased by 121%, 113% and 138% over that of room temperature, but was lower than when withstanding heat 700 °C. At 700 °C and beyond, many cracks combined with each other, causing the peak strains to become gentler and then gradually subside.

Fig. 10 reveals that steel fiber content did not significantly affect the peak strains from room temperature to 200 °C. However, when temperatures exceeded 200 °C, higher steel fiber content generally indicated a higher peak strain. At 800 °C, the overall peak strain subsided substantially. Following regression analysis, peak strain of specimens with different steel fiber content is shown as follows:

$$\frac{\varepsilon_{cT}}{\varepsilon_o} = \begin{cases} 1.043 - 1.483\times10^{-3}T + 1.142\times10^{-5}T^2 - 9.544\times10^{-9}T^3 & V_f = 0.01 \\ 1.129 - 4.177\times10^{-3}T + 2.154\times10^{-5}T^2 - 1.826\times10^{-8}T^3, & V_f = 0.02 \\ 1.066 - 3.012\times10^{-3}T + 1.788\times10^{-5}T^2 - 1.476\times10^{-8}T^3, & V_f = 0.03 \end{cases} \quad 25\,^\circ\mathrm{C} < T \le 800\,^\circ\mathrm{C} \tag{2}$$

where ε_o and ε_{cT} refer to peak strains corresponding to the compressive strength of RPC at room temperature and after high temperatures. For different steel fiber contents, the correlation coefficient R^2 in Eq. (2) was 0.92, 0.92 and 0.90, respectively. Fig. 10 reveals that the analysis model closely corresponded to the test results. In contrast with the peak strain test for conventional concrete after high temperatures by Chang et al. (2006), the peak strain of RPC exceeded that of conventional concrete before heat treatment to 500 °C, but decreased to lower than that of conventional concrete after temperatures exceeded 500 °C. This finding suggests that adding steel fibers in concrete helped to prevent cracks from appearing and expanding.

3.5. Modulus of elasticity

The modulus of elasticity of RPC after high temperatures was found using the ASTM C469 standard test method. According to Table 3 and Fig. 11, a rising temperature decreases the modulus of elasticity rapidly; in addition the rate of decrease decelerates after temperatures exceed 600 °C. The modulus of elasticity of RPCF1, RPCF2 and RPCF3 decreased by 2%, 4% and 2% at 200 °C; at 300 °C; it decreased about 26%, 28% and 34%, i.e. an average decrease of 30%. In the range of 200–300 °C, high temperatures decrease the

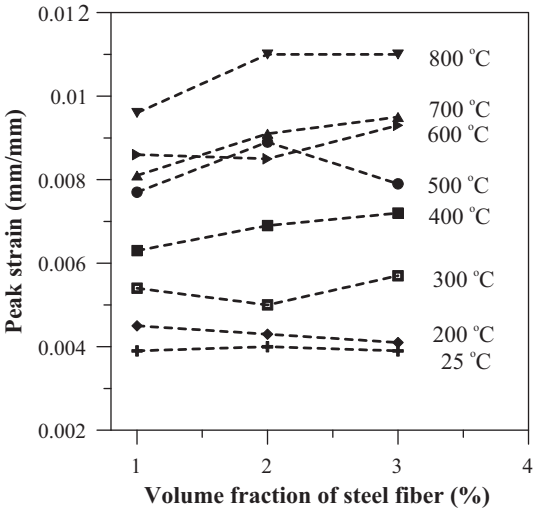

Fig. 10. Peak strain of RPC specimens versus steel fiber content after the different temperatures.

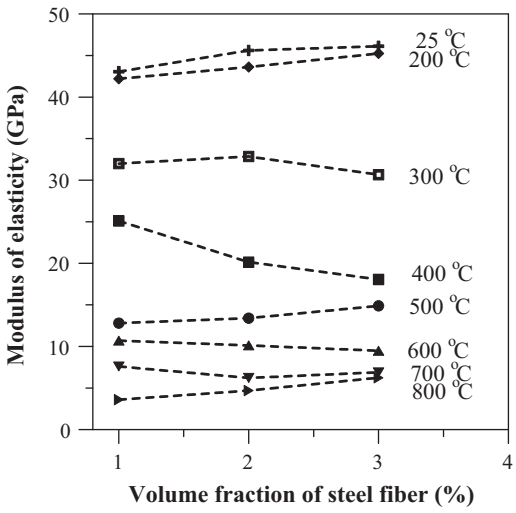

Fig. 12. Modulus of elasticity of RPC specimens versus steel fiber content after the different temperatures.

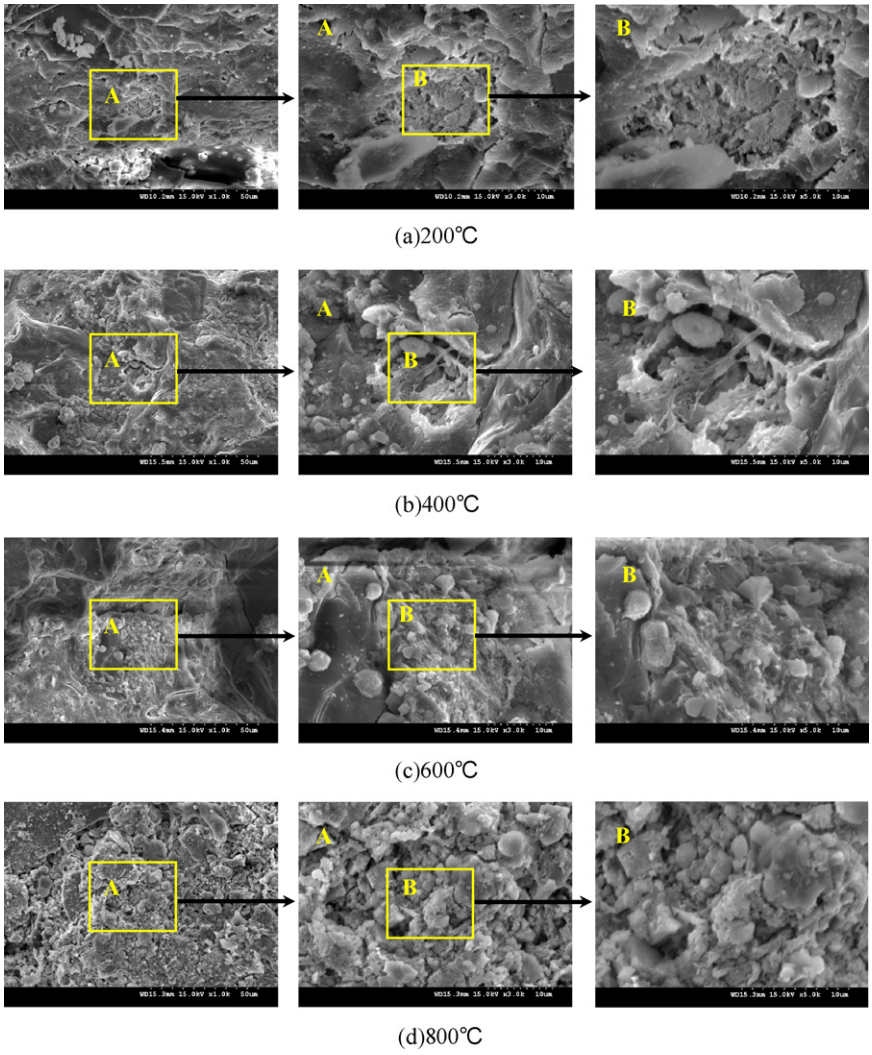

Fig. 13. SEM observations on microstructure of RPC after different high temperatures.

compressive strength of the specimens, increases the peak strain and decreases the modulus of elasticity. At 400 °C, the modulus of elasticity of RPCF1, RPCF2 and RPCF3 decreased to 42%, 56% and 61%, respectively. At 500 °C, the modulus of elasticity of all specimens decreased about 70% over that of room temperature., The modulus of elasticity of RPC specimens declined at a higher rate between 400 and 500 °C owing to the relatively larger decrease in compressive strength and higher deformation. At 600 °C, the modulus of elasticity of RPCF1, RPCF2 and RPCF3 decreased to 75%, 78% and 79%, thus retaining roughly 22% of its original value. At 700 °C, the modulus of elasticity of RPCF1, RPCF2 and RPCF3 decreased about 82%, 86% and 85%, respectively; only roughly 15% of its original value remained. Between 600 and 700 °C, modulus of elasticity decreased by over 80% because high temperatures altered the properties of concrete and softened the steel fibers. At 800 °C, the modulus of elasticity of RPCF1, RPCF2 and RPCF3 decreased by 92%, 90% and 86%; only roughly 10% of their original value remained.

Fig. 12 shows the effect of steel fiber content on modulus of elasticity. In addition to 300 °C and 400 °C, the modulus of elasticity of RPC increased along with steel fiber content for all other temperatures. Following regression analysis, RPC with various steel fiber contents can be expressed using the following equation:

$$\frac{E_{cT}}{E_c} = \begin{cases} 1.011 + 7.21 \times 10^{-4}T - 6.797 \times 10^{-6}T^2 + 5.626 \times 10^{-9}T^3, & V_f = 0.01 \\ 1.026 + 4.181 \times 10^{-4}T - 6.564 \times 10^{-6}T^2 + 5.832 \times 10^{-9}T^3, & V_f = 0.02, \quad 25\,^\circ\text{C} < T \leq 800\,^\circ\text{C} \\ 1.043 - 2.258 \times 10^{-5}T - 5.487 \times 10^{-6}T^2 + 5.2 \times 10^{-9}T^3, & V_f = 0.03 \end{cases} \tag{3}$$

where E_{cT} and E_c represent the modulus of elasticity of RPC at room temperature and after a high temperature. The correlation coefficient R^2 for different V_f values in Eq. (3) is 0.97, 0.97 and 0.96. According to Fig. 12, comparing our results with the modulus of elasticity experiment for conventional concrete after high temperatures by Chang et al. (2006) reveals that RPC after high temperatures had a relatively higher modulus of elasticity, making it tougher than conventional concrete.

3.6. Microstructure of RPC

This study analyzes the microstructure of RPC specimen after different high temperatures based on use of a scanning electron microscope (SEM), in which its damaged mechanism was observed while further elucidating the fluctuating patterns of the mechanical properties from a macro perspective. Fig. 13 is the micrograph of

RPC specimen at low and high magnification power showing very dense microstructure. The center portions of the photographed pictures were labeled with A and B for easier observation; the selected magnification power were 1000×, 3000× and 5000×.

Fig. 13(a) displays the microstructure of RPC after heat treatment under 200 °C. At this temperature, silica fume can react with cement hydrates to produce C–S–H; quartz powder serves as a catalyst and accelerates hydration reaction. According to this figure, the C–S–H structure is complete and closely knit, in which only a small portion of the silica fume has not hydrated and is scattered as small grains; the surface is covered by hydration products. At this temperature, hydration products become cemented into a continuous phase; in addition, the overall structure is more even and closely knit, subsequently increasing the compressive strength significantly. Fig. 13(b) illustrates the microstructure of RPC after heating under 400 °C. At this temperature, absorbed water and pore water is gradually lost and C–S–H and calcium silicate hydrates are dehydrated. Additionally, an increasing number of pores is observed and the spiked sphere appearance changes to resemble a coral reef. Moreover, hydration products are no longer closely knit, and the originally cemented continuous phase gradually transforms into a dispersed phase. However, micro structural changes are generally insignificant, making the reduction in overall mechanical properties only marginal. Fig. 13(c) illustrates the microstructure of RPC after withstanding heat treatment under 600 °C, at which temperature, crystal water and cement hydrates begin to dissolve. Cement hydrates generally begin to dissolve at roughly 550 °C, explaining why the specimen strength decreases the most in this temperature range; it is largely attributed to C–H dehydration. Fig. 13(c) reveals that the RPC microstructure loosens, large amounts of irregular rose bush-like structures similar to monosulfate aluminate appear, continuous hydration products decrease in number, the number of cracks increases, and the overall mechanical properties diminish significantly. Fig. 13(d) shows the microstructure of RPC after exposed to heat under 800 °C. The effect of H on the C–H portion caused the layered plate to have many pores and a rough, grainy surface; the number of cracks increased as well. Furthermore, some changes were also observed in the C–S–H. A portion of it was a coral reef structure while some portions melted into a rough surface, leaving the specimen with little residual compressive strength.

4. Conclusions

This study presents a series of experiments to investigate the mechanical properties of RPCs after exposure to high temperatures. The following conclusions are drawn:

(1) The slope of the rising section of the stress–strain curve decreases with increasing temperatures. The front section of RPCF1 and RPCF2 stress–strain curves concaves upwards; the declining section gradually becomes gentler. Additionally, increasing temperatures significantly decreased the peak stress, but increased the peak strain.
(2) The compressive strength of RPC gradually increases when specimens are heated to 200–300 °C, but starts to decrease as temperatures increase continuously. Specimens with 1% steel fiber content have a higher compressive strength between 200 and 400 °C than at room temperature; their compressive strength begins to subside when temperatures exceed 500 °C. Specimens with 2% and 3% steel fiber content significantly increase in compressive strength from 200 to 300 °C; their compressive strength gradually decreases as temperatures reach 400 °C and beyond.
(3) The number of peak strains gradually increases along with temperatures at 200 °C; the number of strains increases the fastest between 400 and 500 °C then gradually decelerates. The increase of peak strains along with steel fiber content does not significantly differ from room temperature to 200 °C. When temperatures exceed 200 °C, a higher steel fiber content generally implies a higher peak strain. At 800 °C, the overall number of peak strains declines substantially.
(4) The modulus of elasticity of RPC rapidly decreases with an increasing temperature, subsequently decelerating after temperatures exceed 600 °C. In addition to 300 °C and 400 °C, a higher steel fiber content implies a higher modulus of elasticity for all other temperatures.

References

Arioz, O., 2007. Effects of elevated temperatures on properties of concrete. Fire Safety Journal 42 (8), 516–522.
Atkinson, T., 2004. Polypropylene fibers control explosive spalling in high performance concrete. Concrete 38 (10), 69–70.
Bayard, O., Plé, O., 2003. Fracture mechanics of reactive powder concrete: material modeling and experimental investigations. Engineering Fracture Mechanics 70 (7–8), 839–851.
Bazant, Z.P., Kaplan, M.F., 1996. Concrete at High Temperature: Material Properties and Mathematical Models. Longman Group Limited, London.
Chan, Y.N., Peng, G.F., Anson, M., 1999. Residual and pore structure of high-strength concrete and normal strength concrete after exposure to high temperature. Cement and Concrete Composites 21 (1), 23–27.
Chan, Y.W., Chu, S.H., 2004. Effect of silica fume on steel fiber bond characteristics in reactive powder concrete. Cement and Concrete Research 34 (7), 1167–1172.
Chang, Y.F., Chen, Y.H., Sheu, M.S., Yao, G.C., 2006. Residual stress–strain relationship for concrete after exposure to high temperatures. Cement and Concrete Research 36 (10), 1999–2005.
Chen, B., Liu, J., 2004. Residual strength of hybrid-fiber-reinforced high-strength concrete after exposure to high temperatures. Cement and Concrete Research 34 (6), 1065–1069.
Cheyrezy, M., Maret, V., Frouin, L., 1995. Microstructural analysis of RPC. Cement and Concrete Research 25 (7), 1491–1500.
El-Dieb, A.S., 2009. Mechanical, durability and microstructural characteristics of ultra-high-strength self-compacting concrete incorporating steel fibers. Materials and Design 30 (10), 4286–4292.
Georgali, B., Tsakiridis, P.E., 2005. Microstructure of fire-damaged concrete. A case study. Cement and Concrete Composite 27 (2), 255–259.
Hammer, T.A., 1992. High strength concrete, Phase 3, SP6 fire resistance-report 6.2, Spalling reduction through material design. SINTEF report STF70 F92156, Trondheim, Norway.
Hannant, D.J., 1978. Fibre Cements and Fibre Concretes. John Wiley & Sons.
Husem, M., 2006. The effects of high temperature on compressive and flexural strengths of ordinary and high-performance concrete. Fire Safety Journal 41 (2), 155–163.
Kalifa, P., Chene, G., Galle, C., 2001. High-temperature behavior of HPC with polypropylene fibres – from spalling to microstructure. Cement and Concrete Research 31 (10), 1487–1499.
Lau, A., Anson, M., 2006. Effect of high temperatures on high performance steel fiber reinforced concrete. Cement and Concrete Research 36 (9), 1698–1707.
Li, M., Qian, C.X., Sun, W., 2004. Mechanical properties of high-strength concrete after fire. Cement and Concrete Research 34 (6), 1001–1005.
Mansur, M.A., Wee, T.H., Chin, M.S., 1995. Derivation of the complete stress–strain curves for concrete in compression. Magazine of Concrete Research 47, 285–290.
Nishida, A., Yamazaki, N., 1995. Study on the properties of high strength concrete with short polypropylene fiber for spalling resistance. In: Proceedings of International Conference on Concrete Under Severe Conditions , CONSEC'95, Sapporo, Japan, pp. 1141–1150.
Noumowé, A., Siddique, R., Ranc, G., 2009. Thermo-mechanical characteristics of concrete at elevated temperatures up to 310 °C. Nuclear Engineering and Design 239 (3), 470–476.
Poon, C.S., Shui, Z.H., Lam, L., 2004. Compressive behavior of fiber reinforced high-performance concrete subjected to elevated temperature. Cement and Concrete Research 34 (12), 2215–2222.
Reis, B.C., Neves, I.C., Tadeu, A.J.B., Rodrigues, C., 2001. High-temperature compressive strength of steel fiber high-strength concrete. Journal of Materials in Civil Engineering 13 (3), 230–234.
Richard, P., Cheyrezy, M., 1994. Reactive powder concretes with high ductility and 200–800 MPa compressive strength. In: Proceedings of V.M. Malhotra Symposium "Concrete Technology. Past, Present and Future" ACI SP 144-24 , P.K. Metha, S. Francisco, pp. 507–518.
Richard, P., Cheyrezy, M., 1995. Composition of reactive powder concretes. Cement and Concrete Research 25 (7), 1501–1511.
Sideris, K.K., Manita, P., Chaniotakis, E., 2009. Performance of thermally damaged fiber reinforced concretes. Construction and Building Materials 23 (3), 1232–1239.
Tai, Y.S., 2009. Flat ended projectile penetrating ultra-high strength concrete plate target. Theoretical and Applied Fracture Mechanics 51 (2), 117–128.

Tai, Y.S., 2009b. Uniaxial compression tests at various loading rates for reactive powder concrete. Theoretical and Applied Fracture Mechanics 52 (1), 14–21.

Wang, Y.H., Wang, Z.D., Liang, X.Y., An, M.Z., 2008. Experimental and numerical studies on dynamic compressive behavior of reactive powder concretes. Acta Mechanica Solida Sinica 21 (5), 420–430.

Zanni, H., Cheyrezy, M., Maret, V., Philippot, S., Nieto, P., 1996. Investigation of hydration and pozzolanic reaction in reactive powder concrete (RPC) using 29Si NMR. Cement and Concrete Research 26 (1), 93–100.

Zhang, Y., Sun, W., Liu, S., Jiao, C., Lai, J., 2008. Preparation of C200 green reactive powder concrete and its static–dynamic behaviors. Cement and Concrete Composites 30 (9), 831–838.